

Electronic Supplementary Information

Uncontinuously covered IrO₂-RuO₂@Ru electrocatalysts for oxygen evolution reaction: How high activity and long-term durability can meet up in the synergistic and hybrid nano-structure?

Guoqiang Li,^{abc} Songtao Li,^d Junjie Ge,^{*ab} Changpeng Liu^{ab} and Wei Xing^{*ab}

*Corresponding author: W. Xing, E-mail: xingwei@ciac.ac.cn

J. Ge, E-mail: gejj@ciac.ac.cn

Tel.: 86-431-85262223; Fax: 86-431-85685653

^a State Key Laboratory of Electroanalytical Chemistry, Changchun Institute of Applied Chemistry, Chinese Academy of Sciences, Changchun 130022, PR China.

^b Laboratory of Advanced Power Sources, Jilin Province Key Laboratory of Low Carbon Chemical Power Sources, Changchun Institute of Applied Chemistry, Chinese Academy of Sciences, Changchun 130022, PR China.

^c University of Chinese Academy of Sciences, Beijing 100039, PR China.

^d Institute of Mathematics, Jilin University, Changchun 130012, PR China

1 Experimental Section

1.1 Materials

The chemical reagent $\text{H}_2\text{IrCl}_6 \cdot x\text{H}_2\text{O}$ (35 wt% Ir) and $\text{RuCl}_3 \cdot 3\text{H}_2\text{O}$ were purchased from Sino-Platinum Metals Co., Ltd. 5 wt% Nafion® ionomer was purchased from DuPont Co. NaBH_4 was purchased from Sinopharm Chemical Reagent Co., Ltd. NaOH , HNO_3 , H_2SO_4 and ethanol solution were purchased from Beijing Chemical Co. and were used as received without further purification. Commercial IrO_2 and RuO_2 (denoted as IrO_2 (CM) and RuO_2 (CM), respectively) were purchased from Alfa Aesar Chemical Co., Ltd. Commercial Pt/C (20 wt%Pt) catalyst was purchased from Johnson Matthey Company. It should be noted that all solutions in our work were prepared using Millipore-MiliQ water (resistivity: $\rho \geq 18 \text{ M}\Omega \cdot \text{cm}$) and the reagents used were analytical-grade.

1.2 Preparation of catalysts

The synthesis of $\text{IrO}_2\text{-RuO}_2@\text{Ru}$ catalysts was proposed and accomplished through the following procedures: taking $\text{IrO}_2\text{-RuO}_2@\text{Ru}$ (1:1) as an example. The preparation of metallic Ru was the first procedure, 0.2 mmol $\text{RuCl}_3 \cdot 3\text{H}_2\text{O}$ was dissolved in distilled water to form a 30 mL solution. Then, 6 mL of aqueous NaBH_4 solution (0.2 M) was quickly injected into the RuCl_3 solution under vigorous stirring. The stirring was continued for about 10 min until the entire solution became colorless. Finally, the metallic Ru was obtained after filtered, washed and dried. Subsequently, the preparation of $\text{IrO}_2\text{-RuO}_2@\text{Ru}$ (1:1) was another procedure. Firstly, 0.2 mmol Ru was dispersed into 40 mL deionized water ultrasonically for 1 h. After that, 0.2 mmol

$\text{H}_2\text{IrCl}_6 \cdot x\text{H}_2\text{O}$ was added to the Ru suspension to react for another 1 h. Then, aqueous NaOH solution (1 M) was added to the aforementioned solution and stirred for 1 h at 80 °C, this complex was precipitated by addition of HNO_3 (1 M) until the pH reached 8. Finally, the $\text{IrO}_2\text{-RuO}_2@\text{Ru}$ (1:1) was achieved by centrifuged, washed, dried and annealed in air at 450 °C for 1 h. Similarly, $\text{IrO}_2\text{-RuO}_2@\text{Ru}$ (2:1), $\text{IrO}_2\text{-RuO}_2@\text{Ru}$ (3:1) and $\text{IrO}_2\text{-RuO}_2@\text{Ru}$ (4:1) were fabricated by varying the atomic ratios of Ir/Ru in the feeding solutions. Moreover, Ir_3RuO_2 alloy oxide and pure IrO_2 were prepared through similar method.

1.3 Physical characterization

The crystallinity and phase purity of the prepared catalysts were confirmed by X-Ray diffraction (XRD) measurements using a Rigaku-D/MAX-PC2500 X-ray diffractometer (Japan) with the Cu Ka (1.5405 \AA) as a radiation source operating at 40 kV and 200 mA. The surface elemental composition and chemical states of as-prepared catalysts were analyzed by X-ray photoelectron spectroscopy (XPS, Kratos Ltd. XSAM-800) with an Al Ka monochromatic source. The specific surface area was determined through N_2 gas adsorption/desorption measurements (ASAP 2020, Micromeritics Instrument Corporation, USA), calculated by the Brunauer-Emmett-Teller (BET) formulations. The morphologies and compositions were characterized with transmission electron microscopy (TEM), high-resolution transmission electron microscopy (HRTEM), high-angle annular dark-field scanning TEM (HAADF-STEM), element mapping analysis and energy-dispersive X-ray spectroscopy (EDX) by Tecnai G2 F20 S-TWIN electron microscope (FEI Company, USA) working at an

accelerating voltage of 200 kV. Inductively coupled plasma optical emission spectroscopy (ICP-OES; X Series 2, Thermo Scientific USA) was used to determine the quantity of Ir, Ru dissolution after the accelerated durability tests.

1.4 Electrochemical measurements

All electrochemical tests were carried out with a Princeton Applied Research Model273 Potentiostat/Galvanostat and a conventional three electrode electrochemical cell at room temperature with 0.5 mol L⁻¹ H₂SO₄ purged with high-purity N₂ as electrolyte solution. A Pt plate was used as the counter electrode and a saturated calomel electrode (SCE) was used as the reference electrode. The potentials in this work were quoted with respect to reversible hydrogen electrode (RHE). In 0.5 M H₂SO₄, $E(\text{RHE}) = E(\text{SCE}) + 0.26 \text{ V}$. The working electrode was a glassy carbon (GC, 4 mm diameter), it was polished with slurry of 0.3 μm and 0.05 μm alumina successively and washed ultrasonically in deionized water prior to use. The working electrode was prepared as follows: firstly, 5 mg of the catalyst was dispersed ultrasonically in 525 μL solutions containing of 25 μL Nafion® solution (5 wt%) and 0.5 mL ethanol solution; secondly, 5 μL catalyst inks was pipetted and spread on the glassy carbon disk; at last, the electrode was obtained after the solvent volatilized with the catalyst loading was 0.379 mg cm⁻². Cyclic voltammetry (CV) curves were recorded in a potential window between 0.30 and 1.40 V, and the scanning rate ranged from 2 to 300 mV s⁻¹ in N₂-saturated solution. The charge (Q) was calculated from the different voltammograms of various scanning rates, by the following equation:

$$Q = \int_{E_1}^{E_2} \frac{|j|}{\nu} dE \quad (1)$$

where j is the current density obtained from CV curves, ν is the scanning rate ranged from 2 to 300 mV s⁻¹, and E is the scanning potential between 0.70 and 1.40 V. Linear sweep voltammetry (LSV) curves for OER were recorded in a potential window between 1.10 and 1.70 V at a potential scanning rate of 5 mV s⁻¹ in N₂-saturated solution at room temperature.

Turnover frequency (TOF) calculation of the catalysts: The TOF value was calculated from the equation^{1,2}:

$$TOF = \frac{j \times A}{4 \times F \times n} \quad (2)$$

where j is the current density at a given potential, A is the surface area of the electrode, F is the Faraday constant (a value of 96485.3 C mol⁻¹), and n is the number of moles of metal on the electrode. All the Ir and Ru atoms were assumed to be accessible for catalyzing the OER.

Ohmic drop was corrected using electrochemical impedance spectroscopy (EIS) methods according to the equation:

$$E_a = E_b - IR_s \quad (3)$$

where E_a is the potential after I - R correction, E_b is the potential before I - R correction, I is the corresponding current and R_s is the resistance of the system obtained from EIS plots as the first intercept of the main arc, all data have been corrected for 90% iR potential drop. The EIS were recorded on an Autolab potentiostat in the frequency range of 0.1 Hz to 10 kHz at the potential of 1.55 V, a 10 mV amplitude of sinusoidal

potential perturbation was employed in the measurements. The chronoamperometric (CA) experiments were performed in N₂-saturated 0.5 M H₂SO₄ solution at 1.60 V to estimate the performance degradation of the catalysts N₂-saturated. The accelerated durability tests (ADTs) were performed to assess the catalyst durability by applying cyclic potential sweeps between 1.10 and 1.70 V at a sweep rate of 50 mV/s for 3000 cycles in N₂-saturated H₂SO₄ solution at room temperature.

Two electrode configuration for overall water splitting tests were performed with the as-prepared anodic catalysts and commercial Pt/C (20 wt%Pt) catalyst were used to catalyze the OER and HER in acidic solution, respectively. The loading of anodic catalysts on the electrode was 1.0 mg cm⁻² and the loading on cathode was 2.0 mg cm⁻². The LSV experiments were performed with a potential window ranged from 0.5 to 3.0 V at a scanning rate of 10 mV s⁻¹ in 0.5 M H₂SO₄ at room temperature.

2 Supplementary Tables and Figures

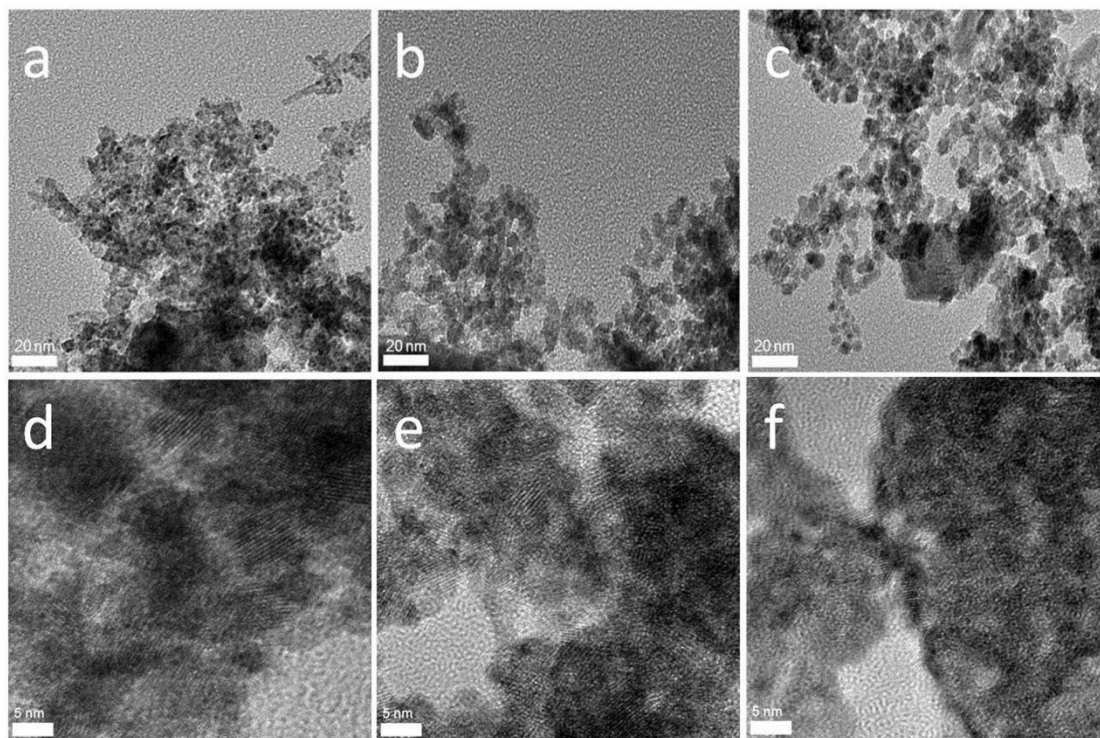


Fig. S1 TEM images and HRTEM images of (a, d) IrO₂-RuO₂@Ru (1:1), (b, e) IrO₂-RuO₂@Ru (2:1) and (c, f) IrO₂-RuO₂@Ru (4:1).

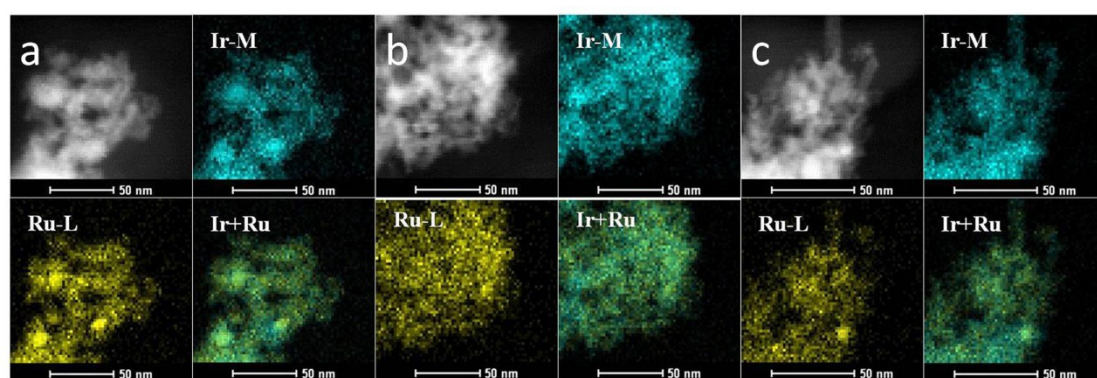


Fig. S2 HAADF and the corresponding elemental mapping images of (a) IrO₂-RuO₂@Ru (1:1), (b) IrO₂-RuO₂@Ru (2:1) and (c) IrO₂-RuO₂@Ru (4:1).

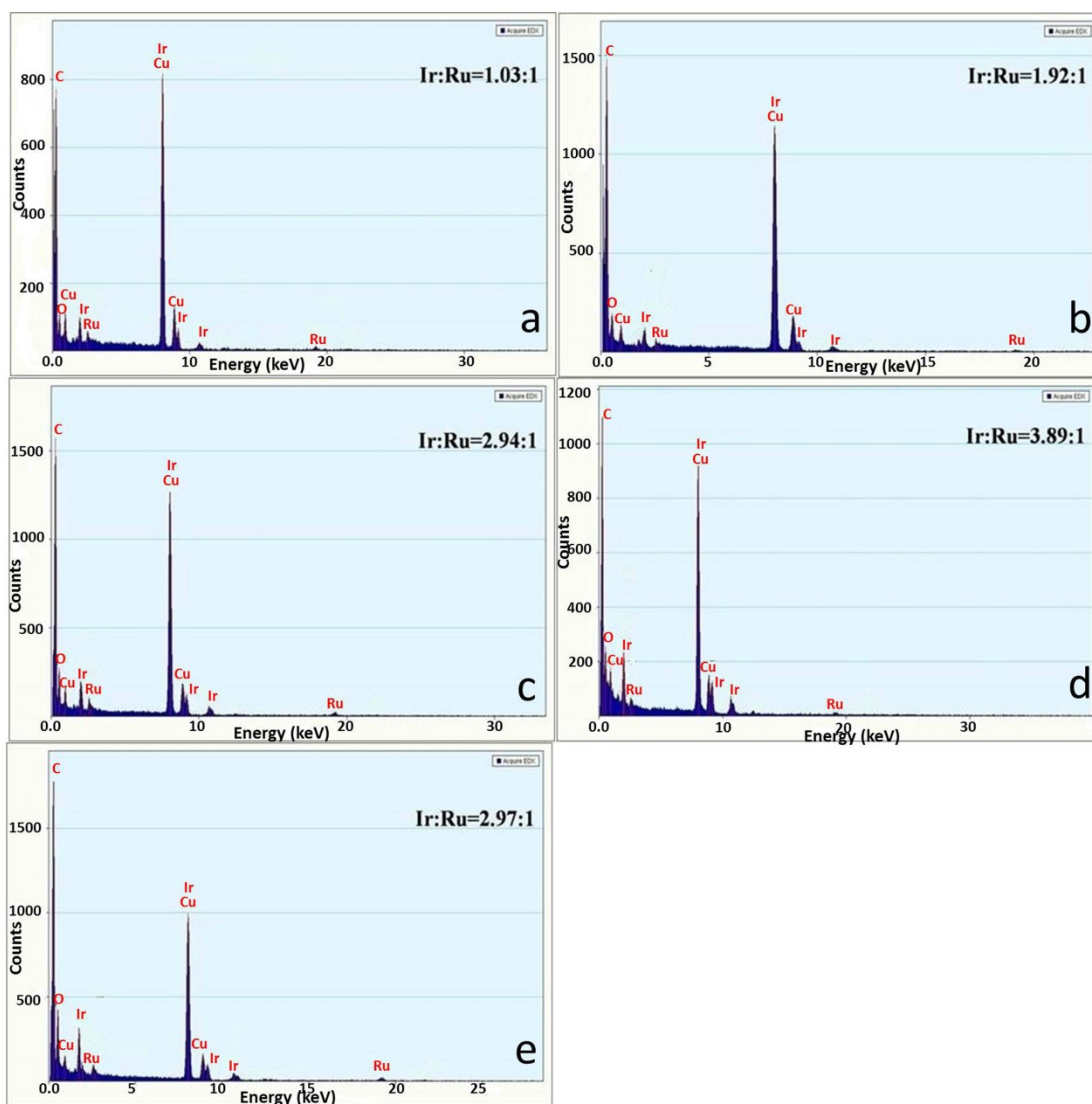


Fig. S3 EDX patterns of (a) IrO₂-RuO₂@Ru (1:1), (b) IrO₂-RuO₂@Ru (2:1), (c) IrO₂-RuO₂@Ru (3:1), (d) IrO₂-RuO₂@Ru (4:1) and (e) Ir₃RuO₂.

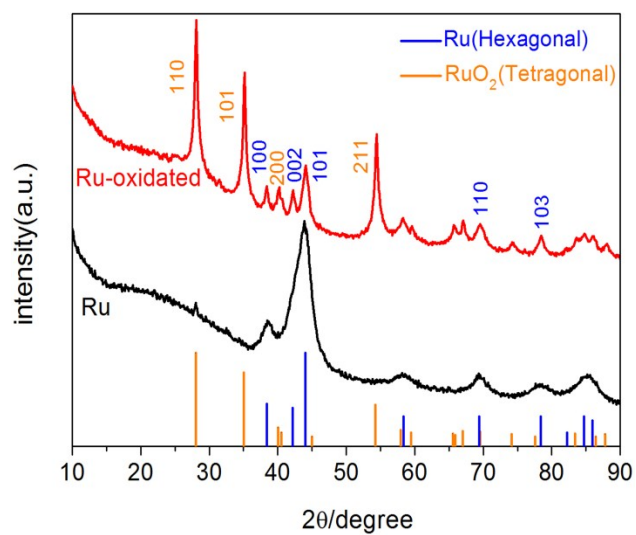


Fig. S4 XRD patterns of metallic Ru and Ru-oxidized after heat treatment under 450

°C in air.

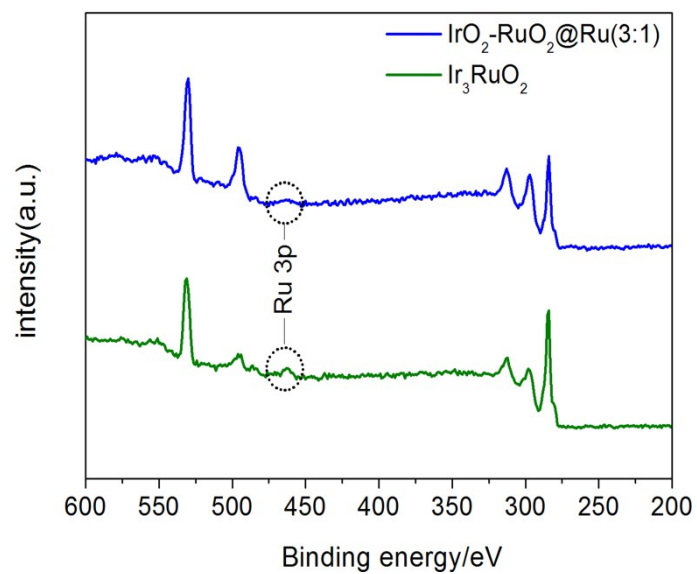


Fig. S5 XPS spectra of $\text{IrO}_2\text{-RuO}_2\text{@Ru(3:1)}$ and Ir_3RuO_2 within the binding energy range between 600 and 200 eV.

Table S1. Theoretical and actual value of Ir:Ru on the surface of IrO₂-RuO₂@Ru (1:1), IrO₂-RuO₂@Ru (2:1), IrO₂-RuO₂@Ru (3:1), IrO₂-RuO₂@Ru (4:1), IrO₂ and Ir₃RuO₂.

Catalyst	Ir:Ru (theoretical value)	Ir:Ru (actual value)
IrO ₂ -RuO ₂ @Ru (1:1)	1:1	9.01:3.14 (2.87)
IrO ₂ -RuO ₂ @Ru (2:1)	2:1	8.17:2.09 (3.91)
IrO ₂ -RuO ₂ @Ru (3:1)	3:1	8.1:1.3 (6.23)
IrO ₂ -RuO ₂ @Ru (4:1)	4:1	9.08:1.37 (6.63)
IrO ₂	---	---
Ir ₃ RuO ₂	3:1	6.14:2.11 (2.91)

Table S2. XPS analysis of IrO₂-RuO₂@Ru (1:1), IrO₂-RuO₂@Ru (2:1), IrO₂-RuO₂@Ru (3:1) and Ir₃RuO₂.

Catalyst	Assignment	Position (eV)	Intensity (%)
IrO ₂ -RuO ₂ @Ru (1:1)	Ru (0)	461.7	31.3
	Ru (IV)-RuO ₂	463.7	68.7
IrO ₂ -RuO ₂ @Ru (2:1)	Ru (0)	461.8	39.0
	Ru (IV)-RuO ₂	463.9	61.0
IrO ₂ -RuO ₂ @Ru (3:1)	Ru (0)	462.2	55.8
	Ru (IV)-RuO ₂	464.4	44.2
Ir ₃ RuO ₂	Ru (0)	462.8	33.1
	Ru (IV)-RuO ₂	464.5	66.9

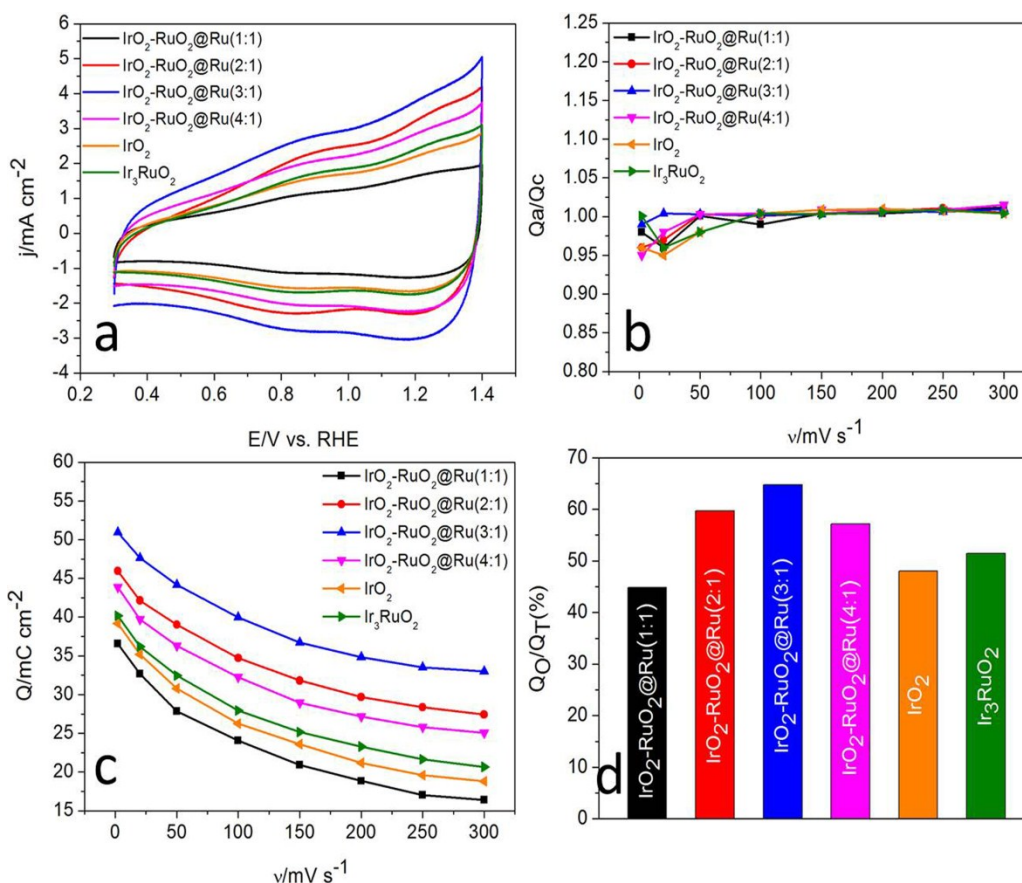


Fig. S6. (a) Cyclic voltammograms at the scanning rate of 50 mV s⁻¹, (b) The reversibility of redox and charging process, (c) Dependence of the voltammetric charges on the scanning rates of 2-300 mV s⁻¹, and (d) The ratios of outer charge to total charge of IrO₂-RuO₂@Ru (1:1), IrO₂-RuO₂@Ru (2:1), IrO₂-RuO₂@Ru (3:1), IrO₂-RuO₂@Ru (4:1), IrO₂ and Ir₃RuO₂ catalysts at the scanning rate of 300 and 2 mV s⁻¹ in N₂ saturated 0.5 M H₂SO₄ at room temperature. Catalyst loading: 0.379 mg cm⁻².

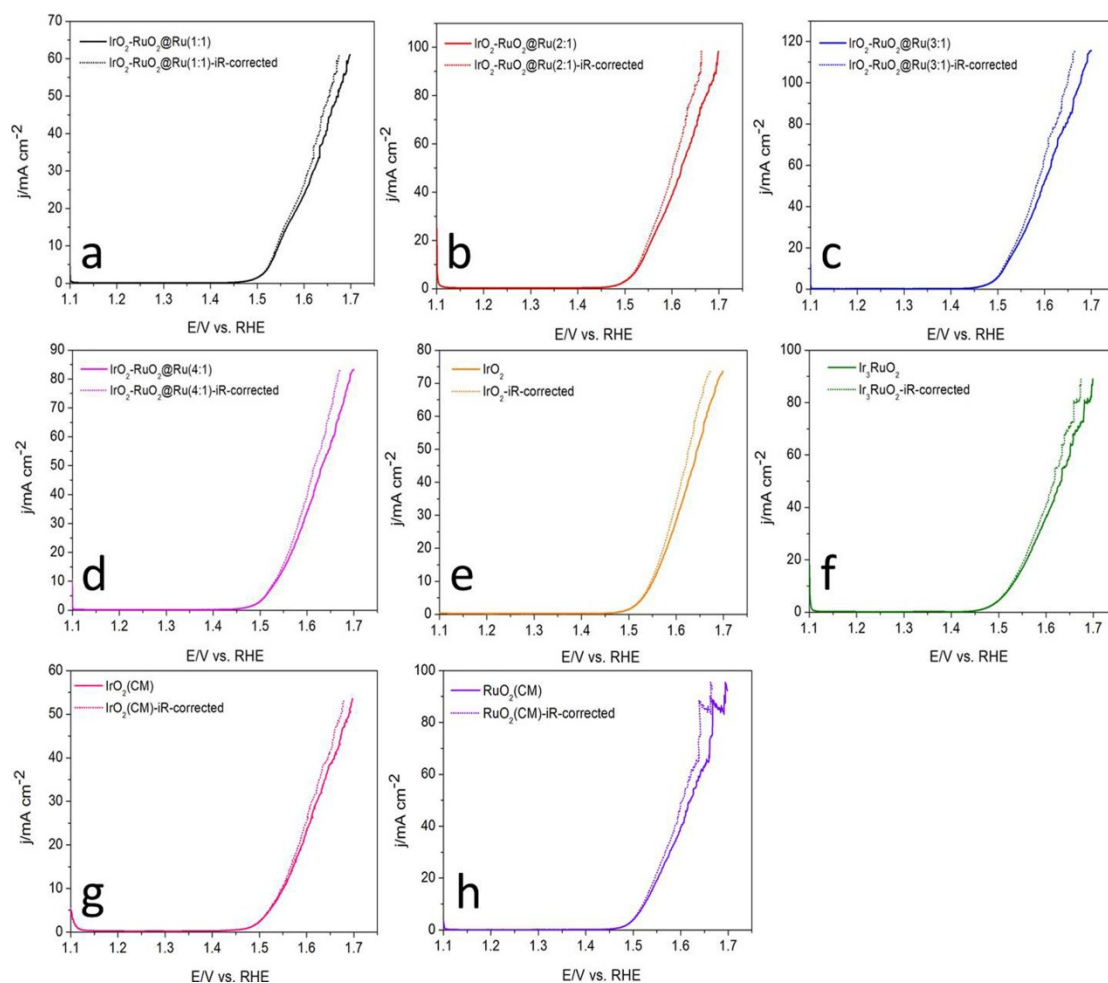


Fig. S7. Linear sweep voltammetry curves of (a) $\text{IrO}_2\text{-RuO}_2\text{@Ru}$ (1:1), (b) $\text{IrO}_2\text{-RuO}_2\text{@Ru}$ (2:1), (c) $\text{IrO}_2\text{-RuO}_2\text{@Ru}$ (3:1), (d) $\text{IrO}_2\text{-RuO}_2\text{@Ru}$ (4:1), (e) IrO_2 , (f) Ir_3RuO_2 , (g) IrO_2 (CM) and (h) RuO_2 (CM) in N_2 saturated 0.5 M H_2SO_4 at room temperature. Catalyst loading: 0.379 mg cm^{-2} . Solid and dashed lines represent polarization curves without and with iR-corrected.

Table S3. Electrocatalytic analysis of linear sweep voltammetry curves.

Catalyst	Overpotential/10 mA cm ⁻²
IrO ₂ -RuO ₂ @Ru (1:1)	312
IrO ₂ -RuO ₂ @Ru (2:1)	299
IrO ₂ -RuO ₂ @Ru (3:1)	281
IrO ₂ -RuO ₂ @Ru (4:1)	301
IrO ₂	317
Ir ₃ RuO ₂	293
IrO ₂ (CM)	318
RuO ₂ (CM)	289

Table S4. Electrocatalytic analysis of linear sweep voltammetry curves for IrO₂-RuO₂@Ru (3:1) and IrO₂ with different catalyst loadings and current densities.

Catalyst	Overpotential/ 0.5 mA cm ⁻²	Overpotential/ 1 mA cm ⁻²	Overpotential/ 5 mA cm ⁻²	Overpotential/ 10 mA cm ⁻²
IrO ₂ -RuO ₂ @Ru (3:1)-0.379 mg cm ⁻²	212	227	267	283
IrO ₂ -RuO ₂ @Ru (3:1)-0.279 mg cm ⁻²	212	234	273	291
IrO ₂ -RuO ₂ @Ru (3:1)-0.179 mg cm ⁻²	223	244	283	304
IrO ₂ -RuO ₂ @Ru (3:1)-0.100 mg cm ⁻²	234	254	295	316
IrO ₂ -RuO ₂ @Ru (3:1)-0.079 mg cm ⁻²	242	260	301	324
IrO ₂ -0.379 mg cm ⁻²	241	261	300	319

Table S5. Comparison of OER overpotential for IrO₂-RuO₂@Ru (3:1) with other electrocatalysts in acidic media.

Catalyst	Electrolyte	Catalyst loading (mg cm ⁻²)	Current density (<i>j</i> , mA cm ⁻²)	Overpotential @ <i>j</i> (mV vs. RHE)	Overpotential @ <i>j</i> (mV vs. RHE; iR-corrected)	References
IrO ₂ -RuO ₂ @Ru (3:1)	0.5 M H ₂ SO ₄	0.379	0.5	211	211	This work
			1	227	227	
			5	268	266	
			10	283	281	
Ir _{0.7} Co _{0.3} O _x	0.5 M H ₂ SO ₄	0.102	0.5	~260	-	3
Ir _{0.67} Sn _{0.3} ₃ O ₂	0.5 M H ₂ SO ₄	0.948	5	25 vs. SCE	-	4
Ru _{0.8} Ir _{0.2} O ₂	0.5 M H ₂ SO ₄	0.38	10	>320	-	5
Ir _{0.5} Ru _{0.5} O ₂	0.5 M H ₂ SO ₄	0.204	10	~320	-	6
IrO _x /SrIrO ₃	0.5 M H ₂ SO ₄	-	10	-	270-290	7
Ir _{0.5} Ru _{0.5} O ₂ /ATO	0.5 M H ₂ SO ₄	0.8	1	-	240	8
IrO ₂ /Nb _{0.05} Ti _{0.95} O	0.5 M H ₂ SO ₄	0.255	1	200-300	-	9
IrO ₂ /Nb-TiO ₂	0.1 M HClO ₄	0.23	10	~310	-	10

Table S6. Electrocatalytic analysis of Tafel plots.

Catalyst	Tafel slope
IrO ₂ -RuO ₂ @Ru (1:1)	55.6 mV/dec
IrO ₂ -RuO ₂ @Ru (2:1)	56.2 mV/dec
IrO ₂ -RuO ₂ @Ru (3:1)	53.1 mV/dec
IrO ₂ -RuO ₂ @Ru (4:1)	56.2 mV/dec
IrO ₂	57.3 mV/dec
Ir ₃ RuO ₂	56.5 mV/dec

Table S7. The quantitative analysis of Ir, Ru dissolution after ADTs by ICP-OES.

Catalyst	Original Ir/Ru ratio(EDX)	Ir-dissolution percentage from Ir component(at%)	Ru-dissolution percentage from Ru component(at%)
IrO ₂ -RuO ₂ @Ru (1:1)	1.03:1	19.8	31.7
IrO ₂ -RuO ₂ @Ru (2:1)	1.92:1	15.4	24.1
IrO ₂ -RuO ₂ @Ru (3:1)	2.94:1	8.3	14.2
IrO ₂ -RuO ₂ @Ru (4:1)	3.89:1	10.6	17.3
IrO ₂	--	12.8	--
Ir ₃ RuO ₂	2.97:1	17.7	28.2

References

1. F. Song and X. Hu, *J. Am. Chem. Soc.*, 2014, **136**, 16481-16484.
2. L. Trotochaud, J. K. Ranney, K. N. Williams and S. W. Boettcher, *J. Am. Chem. Soc.*, 2012, **134**, 17253-17261.
3. W. Hu, H. Zhong, W. Liang and S. Chen, *ACS Appl. Mater. Interfaces*, 2014, **6**, 12729-12736.
4. G. Li, H. Yu, X. Wang, S. Sun, Y. Li, Z. Shao and B. Yi, *Phys. Chem. Chem. Phys.*, 2013, **15**, 2858-2866.
5. N. Mamaca, E. Mayousse, S. Arrii-Clacens, T. W. Napporn, K. Servat, N. Guillet and K. B. Kokoh, *Appl. Catal. B*, 2012, **111-112**, 376-380.
6. L-E. Owe, M. Tsykin, K. S. Wallwork, R. G. Haverkamp and S. Sunde, *Electrochim. Acta*, 2012, **70**, 158-164.
7. L. C. Seitz, C. F. Dickens, K. Nishio, Y. Hikita, J. Montoya, A. Doyle, C. Kirk, A. Voivodic, H. Y. Hwang, J. K. Nørskov and T. F. Jaramillo, *Science*, 2016, **353**, 1011-1014.
8. A. T. Marshall and R. G. Haverkamp, *Electrochim. Acta*, 2010, **55**, 1978-1984.
9. W. Hu, S. Chen and Q. Hua, *Int. J. Hydrogen. Energy*, 2014, **39**, 6967-6976.
10. C. Hao, H. Lv, C. Mi, Y. Song and J. Ma, *ACS. Sustainable Chem. Eng.*, 2016, **4**, 746-756.